Available online at www.sciencedirect.com

ScienceDirect

www.elsevier.com/locate/jes

JES JOURNAL OF ENVIRONMENTAL SCIENCES

www.jesc.ac.cn

Do trace metal(loid)s in road soils pose health risks to tourists? A case of a highly-visited national park in China

*Jingling Huang, Yuying Wu, Yanyao Li, Jiaxun Sun, Yujing Xie, Zhengqiu Fan**

Department of Environmental Science and Engineering, Fudan University, Shanghai 200433, China

ARTICLE INFO

Article history:
Received 11 October 2020
Revised 28 February 2021
Accepted 28 February 2021

Keywords:
Trace metal(loid)s
Pollution assessment
Source apportionment
Health risk assessment
National park

ABSTRACT

Nowadays, more people tend to spend their recreational time in large national parks, and trace metal(loid)s in soils have attracted long-term attention due to their possible harm to human health. To investigate the pollution levels, potential sources and health risks of trace metal(loid)s in road soils, a total of eight trace metal(loid)s (including As, Cd, Cr, Cu, Ni, Pb, Zn and Hg) from 47 soil samples along roads were studied in the Huangshan National Park in Southeast China. The results showed that the concentrations of As, Cd, Pb, Zn and Hg appeared different degrees of pollution compared with their corresponding background values. According to the pollution indices, Hg and Cd were recognized as significant pollutants presenting moderate to high ecological risk. Combining principal component analysis and positive matrix factorization model, the results showed that traffic, industrial, agricultural and natural sources were the potential origins of trace metal(loid)s in this area, with contribution rates of 39.93%, 25.92%, 10.53% and 23.62%, respectively. Non-carcinogenic risks were all negligible, while the carcinogenic risk of As was higher than the limit (1×10^{-6}). Moreover, children were more susceptible to trace metal(loid)s by ingestion which appeared to be a more important exposure pathway than dermal contact and inhalation. The contribution rates of different sources to non-carcinogenic risks and carcinogenic risks were similar among children and adults, while traffic and industrial sources have a significant impact on health risks. This study will give more insights to control the environmental risks of trace metal(loid)s in national parks.

Introduction

Soil supports all forms of terrestrial life (Memoli et al., 2019) and is generally regarded as the most vulnerable part of the environment to trace metal(loid) accumulation (Marchand et al., 2011; Mazurek et al., 2017). As one of the main inorganic pollutants in soils, trace metal(loid)s are natural elements in bedrock (Cheng et al., 2014), mainly derived from geochemical weathering and human activities, such as vehicle exhaust, agriculture fertilizers and industrial activities (Chen et al., 2019; Yang et al., 2019). Due to their high stability, toxicity and accumulation in food chain, trace metal(loid)s in soils can pose significant threats to soil ecosystem, animal

* Corresponding author.
E-mails: zhqfan@fudan.edu.cn, 18210740006@fudan.edu.cn (Z. Fan).

https://doi.org/10.1016/j.jes.2021.02.032
1001-0742/

life and human health (Zhang et al., 2018b), even lead to carcinogenic and chronic diseases (Khan et al., 2016). Recently, trace metal(loid) pollution in soil has become a critical environmental issue that needs urgently to be resolved in the world (Jin et al., 2019).

National parks play an important role in protecting the quality of environment and facilitating the development of recreation and tourism (Memoli et al., 2019; Yaşar Korkanç, 2014). Unfortunately, they are also one of the most susceptible recipients of trace metal(loid) contaminant and have attracted the attention of the global public (Hamad et al., 2019; Mazurek et al., 2017; Mrimi et al., 2019). Trace metal(loid)s accumulated in park soils can be easily transferred to the human body by inhalation, ingestion or dermal absorption pathways (Wu et al., 2019), and accumulate in adipose tissue ultimately affecting organ functions (such as destroying the nervous and endocrine systems). Nowadays, with the improvement of economic level, more and more people choose to spend their leisure time in national parks, which greatly increases their exposure risks to trace metal(loid)s in soils. For children who often go to the park, they may be more vulnerable to trace metal(loid) pollution than adults (Bocca et al., 2004; Gu et al., 2017; Waisberg et al., 2003). Recently, researches on trace metal(loid) pollution in soils are mainly concentrated in mining areas (Irzon et al., 2018), agricultural regions (Yang et al., 2019), large cities (Zhang et al., 2019), industrial estates (Gao and Wang, 2018; Li et al., 2020) or urban parks (Hung et al., 2018), but few studies involve the national parks far from a city. The topsoils of national park roads are most likely to be exposed to tourists (Memoli et al., 2019), so there is an urgent need to explore the human health risks caused by trace metal(loid)s. However, these risks are often underestimated or ignored.

A comprehensive method to evaluate the accumulation and contamination of trace metal(loid)s in soil is greatly important for national parks, which based on the use of appropriate pollution assessment indices to determine the pollution status and identify ecological risks (Elmira et al., 2019; Gasiorek et al., 2017; Gu et al., 2016; Hakanson, 1980; Weissmannová and Pavlovský, 2017; Zhang et al., 2018a). Recently, research has gradually focused on quantifying pollution levels in different situations and identifying the sources of soil pollutants (Tian et al., 2018). To effectively reduce soil trace metal(loid) contamination and the cost of soil remediation, it is essential to apportion the sources in road soils of national parks. Many studies have used multivariate statistical methods for source identification such as Absolute principal component scores-Multivariate linear regression (APCS-MLR), Cluster analysis (CA) and Principal component analysis (PCA) to qualify the sources of soil contaminants. While fewer studies focused on the quantitative receptor models like Chemical mass balance (CMB) and Positive matrix factorization (PMF) to quantify the sources of soil contaminants (Caeiro et al., 2005; Paatero and Tapper, 1993; Zhang et al., 2018a). In this study, to effectively apportion the sources of trace metal(loid)s, a combination of qualitative and quantitative analysis was used. First, PCA and correlation analysis were applied to preliminarily identify the sources of trace metal(loid)s, and then PMF further quantified the types and contribution rates of the sources based on previous results (Zhang et al., 2018b).

Huangshan National Park, located in the more developed southeastern region of China, attracted a total of 3.5 million tourists in 2019 due to its excellent ecological environment and landscape. However, in recent years, the rapid development of the industries around the park has raised concerns that it may be affected by the surrounding pollutants. Therefore, taking Huangshan National Park as a research case, the main research objectives of this study were to explore: (1) What are the pollution status and spatial distribution of trace metal(loid)s in this study area? (2) How to identify potential pollution sources of trace metal(loid)s and quantify their respective contributions? (3) Whether tourists suffered from health risks posed by trace metal(loid)s in road soils of the park?

1. Materials and methods

1.1. Study area

Huangshan National Park (118°6′E - 118°13′E, 30°4′N - 30°11′N), with an area of 160.6 km^2, is in the southeastern Yangtze River Economic Zone which is one of the most developed regions in China. It is located on the southern margin of the northern subtropical zone, with an altitude of 238–1864 m, an average annual temperature of 16.3 °C, and an average annual precipitation of 2394.4 mm. The vegetation type is mainly evergreen broad-leaved forest with a forest coverage rate of 98.29%. The soil is generally acidic, mainly composed of yellow-red soil and yellow soil, and rich in organic matter. The soil matrix is usually granite and quartzite, with obvious horizontal and vertical zonal characteristics. This park has been included in the World Cultural and Natural Heritage List as a World Geopark by the United Nations Educational Scientific and Cultural Organization (UNESCO), and rated as a national 5A scenic area by the National Tourism Administration of China, which has increased more interest and attention to the quality of this area.

In fact, surrounded by numerous densely populated municipalities, Huangshan National Park is the largest and most visited national park in the southeastern region of China and has witnessed rapid economic and tourism development, which caused soil environment threatened by various contaminants such as trace metal(loid)s. In addition, the study area is surrounded by many famous tea-producing areas in China, with a long history of tea planting and extensive use of pesticides and fertilizers (Jiang, 2019). Meanwhile, due to the rich coal and mineral resources in the study area, some mining activities were carried out in the early years, but they have now been stopped.

1.2. Soil sampling and chemical analysis

Tourists mostly visit the park along roads, and roads were considered as the most likely potential places for people to be exposed to trace metal(loid)s in park (Memoli et al., 2019). A total of 47 soil samples (0–20 cm depth) were collected along the main roads in the study area, excluding those roads with less impact on tourists such as cableways and highways. The

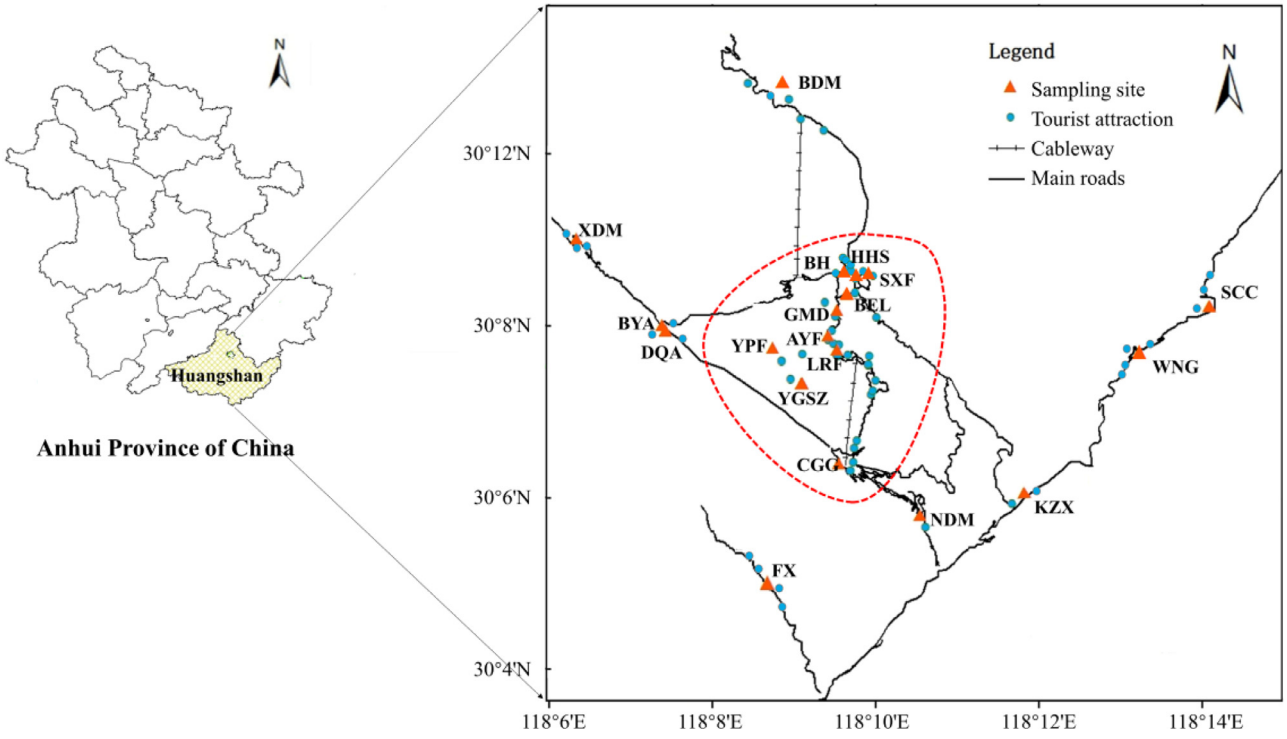

Fig. 1 – Location of the study area and sampling groups. The area inside red curve represents the core scenic area.

adjacent sampling sites were divided into 19 tourist aggregation groups (Fig. 1), and based on the density of traffic and tourist attractions, the 19 sampling groups were further divided into the core scenic areas (including the group of BEL, YGSZ, YPF, LRF, AYF, GMD, BH, HHS, SXF and CGG) and the non-main scenic areas (including the group of FX, DQA, NDM, BYA, XDM, BDM, SCC, WNG and KZX). The exact locations of sampling sites were recorded by GPS.

Each sample was a composite of five sub-samples of equal weight. Sub-samples were collected from five locations from a nearby 1 m^2 area (Appendix A Fig. S1) with a stainless steel hand auger according to the method of GB/T 36197–2018 issued by the Standardization Administration of China. Then, these sub-samples were completely mixed and reduced by quartering (Appendix A Fig. S1) to obtain an aggregate soil sample of about 1 kg. After each sampling, we used tissue paper to remove the soil in contact with the sampler and washed the sampler with distilled water to avoid cross-contamination. Samples were kept in polyethylene bags, numbered and marked separately, and then transported to the laboratory.

In laboratory, all soil samples were air-dried, ground, sieved and digested before analyses. Chemical analyses and quality control were conducted in accordance with the Technical Specifications for Soil Environmental Monitoring of China (HJ/T 166–2004). Soil pH was measured by pH vale meter (pHs-3C, Leici, China), soil dry weight (dw) was measured by analytical balance (XP105DR, Mettler, Switzerland), organic matter (OM) and cation exchange capacity (CEC) were determined by titration. Total nitrogen (TN) was measured by spectrophotometer (UV2501, Shimadzu, Japan), while available potassium concentration was measured by flame photometer (HAD-FP6400A, Shanghai Precision Instrument, China). After digesting the samples, concentrations of Cd, Cr, Cu, Ni, Pb, and Zn were measured by ICP Spectrometer (ICPMS-7900, Thermo Fisher, USA), while As and Hg were measured by atomic fluorescence spectrometer (AFS-8220, Beijing Titan Instruments, China). The detection limits of As, Cd, Cr, Cu, Ni, Pb, Zn and Hg were 0.5, 0.01, 0.1, 0.1, 0.1, 0.1, 0.5 and 0.05 mg/kg, respectively. The relative standard deviations (RSD) for soil properties of duplicates were < 3%.

1.3. *Evaluation methods of pollution*

For the comprehensive assessment of soil pollution degree in the study area, four indices including Geo-accumulation index (I_{geo}), Nemerow index ($PI_{Nemerow}$), Potential ecological risk index (RI) and Pollution load index (PLI) were calculated, and the calculation formulas, parameters and classification criteria of the indices are shown in Table 1. These indices allow to assess the degree of soil pollution with individual trace metal(loid)s (I_{geo}, PI), holistic evaluation of soil quality (IPI, PLI), and the assessment of the ecological risk (RI). Hierarchical cluster analysis (HCA) heat map was integrated to spatially estimate pollution status and potential threats caused by trace metal(loid)s.

1.4. *Source apportionment methods*

The PMF model is one of the receptor models recommended by the USEPA for source apportionment, first proposed and developed based on the previous studies of Paatero Paatero, 1994, 1997; Paatero and Tapper, 1993). It has a wide range of appli-

Table 1 – Calculation formulas, parameters and classification criteria of the pollution indices used in this study.

Indices	Formula	Parameters description	classification criteria
Geo-accumulation index (I_{geo})	$I_{geo} = \log_2[C_i/(k \times B_i)]$	C_i - content of measured metal(loid) i in the samples, B_i - the geochemical background values of metal(loid) i in sedimentary rocks (ordinary shale), k - coefficient, generally taken to be 1.5, is introduced to minimize the possible variations in the background values due to lithogenetic origins.	$I_{geo} \leq 0$, practically unpolluted (Class 0); 0–1, unpolluted to moderately polluted (Class 1); 1–2, moderately polluted (Class 2); 2–3, moderately to heavily polluted (Class 3); 3–4, heavily polluted (Class 4); 4–5, heavily to extremely polluted (Class 5); $I_{geo} > 5$, extremely polluted (Class 6).
Potential ecological risk index (RI)	$C_f^i = C^i/C_n^i$ $E_r^i = T_r^i \times C_f^i$ $RI = \sum_{i=1}^{m} E_r^i$	C_f^i - pollution coefficient of metal(loid) i, C_n^i - regional background value of metal(loid) i (centre, 1990), E_r^i - single potential ecological risk of metal(loid) i, T_r^i - toxicity response parameter (toxicity coefficient) of metal(loid) i (Hakanson, 1980), RI - comprehensive potential ecological risk index.	$E_r^i < 40$, RI <150, low risk; $40 \leq E_r^i < 80$, $150 \leq$ RI <300, moderate risk; $80 \leq E_r^i < 160$, $300 \leq$ RI < 600, considerable risk; $160 \leq E_r^i < 320$, $600 \leq$ RI < 1200, high risk; $E_r^i \geq 320$, RI$\geq$1200, extreme risk.
Nemerow pollution index ($PI_{Nemerow}$)	$PI = C_i/S_i$ $IPI = \sqrt{(P_{max}^2 + \bar{P}^2)/2}$	PI - single pollution index of particular trace metal(loid), S_i - standard value of soil environmental quality, IPI - integrated pollution index, P_{max} - maximum value of the single pollution index of the trace metal(loid), $\bar{P}$ - mean value of the single factor index.	PI $\leq$0.5, unpolluted (Class 0); 0.5 $<$ PI $\leq$ 1, unpolluted to moderately polluted (Class 1); 1 $<$ PI $\leq$ 2, moderately polluted (Class 2); 2 $<$ PI $\leq$ 3, moderately to heavily polluted (Class 3); PI $>$ 3, heavily polluted (Class 4). Besides, IPI $<$ 0.7, safety; 0.7 $\leq$ IPI $<$ 1.0, precaution; 1 $\leq$ IPI $<$ 2, slightly polluted; 2 $\leq$ IPI $<$ 3, moderately polluted; IPI $\geq$ 3, seriously polluted.
Pollution load index (PLI)	$PLI_i = (C_f^1 \times C_f^2 \times C_f^3 \times \cdots \times C_f^n)^{1/n}$ PLI for a zone $= (PLI_1 \times PLI_2 \times PLI_3 \times \cdots \times PLI_n)^{1/n}$		PLI $<$ 1, not polluted; PLI $>$ 1, polluted; PLI $=$ 1, baseline levels of pollution

cation in the identification of trace metal(loid) sources in soil recently due to the non-negative source contribution of each data point and the apportionment of source factor contributions to each trace metal(loid) (Guan et al., 2018; Huang et al., 2018; Li and Feng, 2012). The optimal factor profiles and factor contributions are obtained by the PMF model that minimizes the objective function Q. The concentration matrix X_{ij} and function Q can be calculated by Eqs. (1)-((2):

$$X_{ij} = \sum_{k=1}^{p} g_{ik} f_{kj} + e_{ij} \quad (1)$$

$$Q = \sum_{i=1}^{n} \sum_{j=1}^{m} \left[(x_{ij} - \sum_{k=1}^{p} g_{ik} f_{kj})/u_{ij} \right]^2 \quad (2)$$

where, i and j are the number of samples and trace metal(loid)s, respectively. X_{ij} (mg/kg) is the concentration matrix of trace metal(loid) j in sample i, g_{ik} (mg/kg) is the contribution of source k on sample i, f_{kj} is the contribution of source k on trace metal(loid) j, e_{ij} is the modeling error on the concentration of trace metal(loid) j in sample i, and u_{ij} is the uncertainty of trace metal(loid) j in sample i. PMF v5.0 requires two input files including concentration data and uncertainty data, and the uncertainty (Unc) of the concentration was calculated as Eqs. (3)-(4):

$$\text{Forc} \leq \text{MDL}, \text{Unc} = \frac{5}{6}\text{MDL} \quad (3)$$

$$\text{Else, Unc} = \sqrt{(\text{Error fraction} \times c)^2 + (\text{MDL}/2)^2} \quad (4)$$

Here, c (mg/kg) is the concentration of trace metal(loid)s, MDL is the species-specific method detection limit, Error fraction is a percentage of the measurement uncertainty.

1.5. *Human health risk assessment model*

Human health risks caused by exposure to trace metal(loid)s contained in contaminated road soils mainly occur through three pathways including inhalation, ingestion and dermal contact. The risks caused through ingestion and dermal pathways can be estimated by the average daily dose (ADD_{ingest}, ADD_{dermal}, respectively, mg/(kg•day)), while risk through inhalation can be estimated by the concentration of the chemical in air as the exposure metric ($C_{air\text{-}inhal}$, mg/m^3). They are

calculated as Eqs. (5)-(7):

$$C_{air-inhal} = c \times EF \times ED/PEF \times AT \quad (5)$$

$$ADD_{ingest} = \left[\left(c \times R_{ingest} \times EF \times ED\right)/(BW \times AT)\right] \times 10^{-6} \quad (6)$$

$$ADD_{dermal} = [(c \times SA \times SL \times ABF \times EF \times ED)/(BW \times AT)] \times 10^{-6} \quad (7)$$

The parameters and the real data for Chinese people that were used in Eqs. (5)-(7) are defined in Appendix A Table S1. For the non-cancer risk, HQ_i is the hazard quotient of the i^{th} exposures pathway, and the total hazard indices (HI) is the sum of the hazard quotient (HQ). If the values of HI > 1, it indicates that there are possible adverse health effects. For carcinogenic risk (CR), if the values of CR are greater than 1×10^{-4}, it indicates the carcinogenic risk affects human health, and if CR values are lower than 1×10^{-6}, it means the reverse Huang et al., 2018). They are determined as Eqs. (8)-(11):

For ingestion and dermal pathways,

$$HI = \sum HQ_i = \sum ADD_{ij}/RfD_{ij} \quad (8)$$

$$CR = \sum ADD_{ij} \times SF_{ij} \quad (9)$$

For inhalation pathway,

$$HI = \sum HQ_i = \sum C_{air}/RfC_{ij} \quad (10)$$

$$CR = \sum IUR \times C_{air} \times 10exp(6) \quad (11)$$

The corresponding reference dose (RfD), slope factors (SF) inhalation reference concentration (RfC), and Inhalation Unit Risk (IUR) values from the literature are shown in Appendix A Table S2.

1.6. Statistical analysis

The descriptive statistical parameters and principal components analysis (PCA) were calculated by IBM SPSS v26.0 (IBM, USA). Box plots of I_{geo} and PI were conducted by Origin 2018 (ESRI, US) to determine the data dispersion. The analysis results of the heat map with cluster correlations among sampling sites were visualized by the Heatmap Illustrator v1.0, based on the average concentration for each metal(loid). PMF analysis was conducted with the PMF v5.0 (USEPA, USA). The concentration data and uncertainty data related to these trace metal(loid)s in road soils were input to the PMF model. All those trace metal(loid)s with a signal-to-noise ratio (S/N) defined as "strong". The factor numbers for PMF were set to 3, 4, 5 and 6, respectively. With start seed number chosen randomly, the PMF model was run 20 times. The most appropriate factor number was selected by judging the most stable and smallest Q true value, and the last five factors were the optimal numbers. Moreover, their residuals were between −3 and 3.

2. Results and discussions

2.1. Trace metal(loid) concentrations and distributions in road soils

2.1.1. Descriptive statistics of soil properties and trace metal(loid)s

Several soil parameters (including pH, dry weight, organic matter, cation exchange, total nitrogen and available potassium) were investigated, and the basic statistical summary (e.g. minimum, maximum, mean, median) was presented in Appendix A Table S3. The mean pH value of the study area was 4.57, which was lower than that of the average local background with a value of 6.3 (Appendix A Table S3). Previous studies have found that the lower the soil pH, the lower the binding capacity of trace metal(loid)s (Gąsiorek et al., 2017; Meharg, 2011). It is obvious that soil in this study area was generally acidic, which may lead to a high concentration of soluble trace metal(loid)s. The mean and median concentrations of soil organic matter (SOM) in the study area were 59.53 and 52.30 g/kg, respectively, which were much higher than the local background value of soils in Anhui Province of China (20.0 g/kg) (Appendix A Table S3). Because SOM involves the solid-liquid equilibrium constant (K_p) of trace metal(loid)s, it can affect the mobility and bioavailability of trace metal(loid)s (Center, 1990). Cation exchange (CEC) can affect the migration and enrichment of trace metal(loid)s in soils and the mean value of CEC in the study area was 14.16, indicating that soil preservation capacity was at the intermediate level. In addition, the results also showed that the total nitrogen level (TN) was relatively high, with a mean value of 2.74 g/kg, and soil available potassium content was moderate, with a mean value of 86.00 mg/kg.

As shown in Table 2, all mean element concentrations were in accordance with the Chinese soil guideline (GB 15618–1995) and increased in the following order: Hg (0.14 mg/kg) < Cd (0.29 mg/kg) < Ni (12.22 mg/kg) < As (13.68 mg/kg) < Cu (14.83 mg/kg) < Cr (23.63 mg/kg) < Pb (40.93 mg/kg) < Zn (77.89 mg/kg). Obviously, among all elements, the mean concentrations of As, Cd, Pb, Zn and Hg in this study were higher than their corresponding background values in Anhui Province of China (8.4 mg/kg, 0.084 mg/kg, 26 mg/kg, 58.6 mg/kg, 0.028 mg/kg, respectively). In addition, the mean values of surface enrichment for these elements were significantly greater than 1 (1.63 for As, 3.45 for Cd, 1.57 for Pb, 1.33 for Zn and 5.00 for Hg, respectively). In particular, the mean concentrations of Cd and Hg presented at 3.45 and 5.00 times of their local average background values (0.084 mg/kg and 0.065 mg/kg, respectively), suggesting that soil in the study area has been mildly polluted by anthropogenic activities (Jiang et al., 2017). Comparing to other national parks of the world, the trace metal(loid) concentrations of this study area were at a low or moderate level. The mean Pb concentration (40.93 mg/kg) in this study was relatively higher than that of other national parks, such as the parks in Iraq (16.22 mg/kg), Poland-Roztocze (19.64 mg/kg), Montenegro (27.97 mg/kg), China-Xixi (39.20 mg/kg) and Spain (36.71 mg/kg). The mean concentrations of Cd, Zn and Hg were at the lower middle level, meanwhile the concentrations of Cr, Cu and Ni were rel-

Table 2 – Statistical summary of trace metal(loid)s concentrations (mg/kg) in surface soils.

Country	Park name	Year	Sample size	Depth (cm)		As	Cd	Cr	Cu	Ni	Pb	Zn	Hg	Reference
China	Huangshan National Park	2020	47	0–20	Mean	13.68	0.29	23.63	14.83	12.22	40.93	77.89	0.14	This study
					Min	1.90	0.10	7.30	2.90	2.70	16.20	26.30	0.08	
					Max	51.70	0.72	50.20	60.70	39.10	77.60	161.00	0.36	
					S.D. [a]	8.74	0.14	12.22	13.70	10.06	16.75	30.57	0.06	
Poland	Ojców National Park	2019	23	0–8	Mean	n/a	3.12	n/a	n/a	n/a	158.03	217.49	0.20	Mazurek et al., 2019
Iraq	Halgurd-Sakran National Park	2019	9	0–20	Mean	7.00	n/a	291.55	63.33	328	16.22	116.44	n/a	Hamad et al., 2019
Poland	Roztocze National Park	2017	32	O horizon	Mean	n/a	n/a	16.88	20.49	12.28	19.64	61.52	n/a	Mazurek et al., 2017
Turkey	Kizildag National Park	2017	24	0–25	Mean	n/a	n/a	260	29.90	2935	n/a	120.70	n/a	Saglam, 2017
Poland	Słowiński National Park	2014	15	A horizon	Mean	n/a	n/a	n/a	0.09	n/a	n/a	2.90	n/a	Parzych, 2014
Montenegro	Durmitor National Park	2011	16	0–10	Mean	n/a	1.38	n/a	23.37	n/a	27.97	100.77	n/a	Ratko et al., 2011
China	Xixi National Park	2007	11	0–20	Mean	6.30	0.23	64.90	36.80	n/a	39.20	91.50	0.19	Shao et al., 2007
Spain	Donana National Park	1990	19	n/a	Mean	n/a	2.01	n/a	89.68	n/a	36.71	270.06	0.26	Gonzalez et al., 1990
Local ABVs [b]						8.4	0.084	62.6	19.3	28.1	26	58.6	0.028	CNEM, 1990
Average background of China						11.2	0.097	61.0	22.7	26.9	27.3	74.2	0.065	Chen et al., 2015
Chinese soil guideline [c]						30	0.3	150	50	60	70	200	0.5	Chen et al., 2019

[a] Standard deviation,.
[b] the average soil background values of Anhui province, China,.
[c] Chinese National Environmental Quality Standards (GB 15618-1995).n/a: data not available.

atively low, especially for Ni (12.22 mg/kg) which was much lower than the concentrations in parks of Iraq (328.00 mg/kg) and Turkey (2935 mg/kg). Due to the difference in geological backgrounds and human activities, the concentrations of trace metal(loid)s in soils of national parks in different regions vary greatly (Liu et al., 2020).

2.1.2. *Spatial distribution characteristics of trace metal(loid) pollution*

To investigate the spatial distribution of trace metal(loid)s among the sampling sites, the heat maps coupled with visualized hierarchical cluster analysis (HCA) (Li et al., 2015; Wang et al., 2018) were performed and the results were shown in Fig. 2. It was notable that the clustering results were divided into five main groups. In the C1 group, the sites (including GMD, YGSZ, BEL, AYF and BH), located in the western peripheral non-main scenic areas, were clustered together with mainly Hg pollution, and in a smaller extent with Pb, Cd and As pollution. The pesticides and fertilizers applied in the western part of the national park may contribute to the Hg accumulation in road soils (Dong et al., 2017). The sites of group C2 were mainly in the core scenic area with the most tourist attractions, and mainly polluted by Cd and Pb, followed by Zn, As and Hg. Due to the high traffic density in these sites, long-term emission of vehicle exhaust may cause pollutions with Pb, Cd and Zn in the topsoils (Jiang et al., 2017; Zhang et al., 2018b). The sites of C3 group, located in the non-main scenic areas in the eastern periphery, were mainly polluted by Cd and Cu. The C4 cluster consisting of the sites of HHS and SXF also was the central part of the core scenic area. The trace metal(loid) pollution in this study area was the most serious, with hot spots ranging from "orange" to "red", characterized by high Cd and Hg pollution. The concentrations of As, Cu and Cd in the C5 group were higher, which were attributed to the emissions from copper and coal mining areas near the SCC site. However, all sites were basically free of Cr and Ni contamination.

The high concentrations from HCA heat maps indicated that trace metal(loid)s in road soils of the study area were mainly accumulated in the core scenic areas with a high density of tourist attractions and traffic volume, and sparsely distributed in the non-main scenic area of the study area. The adjacent mining area also had a bit of impact. It was obviously found that soils in this area were affected by Cd and Hg pollution to varying degrees, which may be hazardous to human health (Zhang et al., 2018c).

2.2. *Comprehensive assessment of pollution status*

Assessment of pollution status for trace metal(loid)s partly reflects the potential risks to ecosystems. Table 3 showed the mean ± SD values of pollution indices. The Geo-accumulation Index (I_{geo}) assesses the pollution in soils based on the comparison of trace metal(loid) concentrations with the soil geochemical background (Liu et al., 2018). Results of I_{geo} from the highest to the lowest values were: Hg > Cd > Pb > As > Zn > Cu > Cr > Ni. Hg showed the highest pollution level among all trace metal(loid)s, followed by Cd. Except for Hg (1.78), Cd (0.97) and Pb (0.01), the mean I_{geo} values of the other five trace metal(loid)s were all lower than 0, indicating a practically unpolluted level. According to the calculated I_{geo} values, it can be

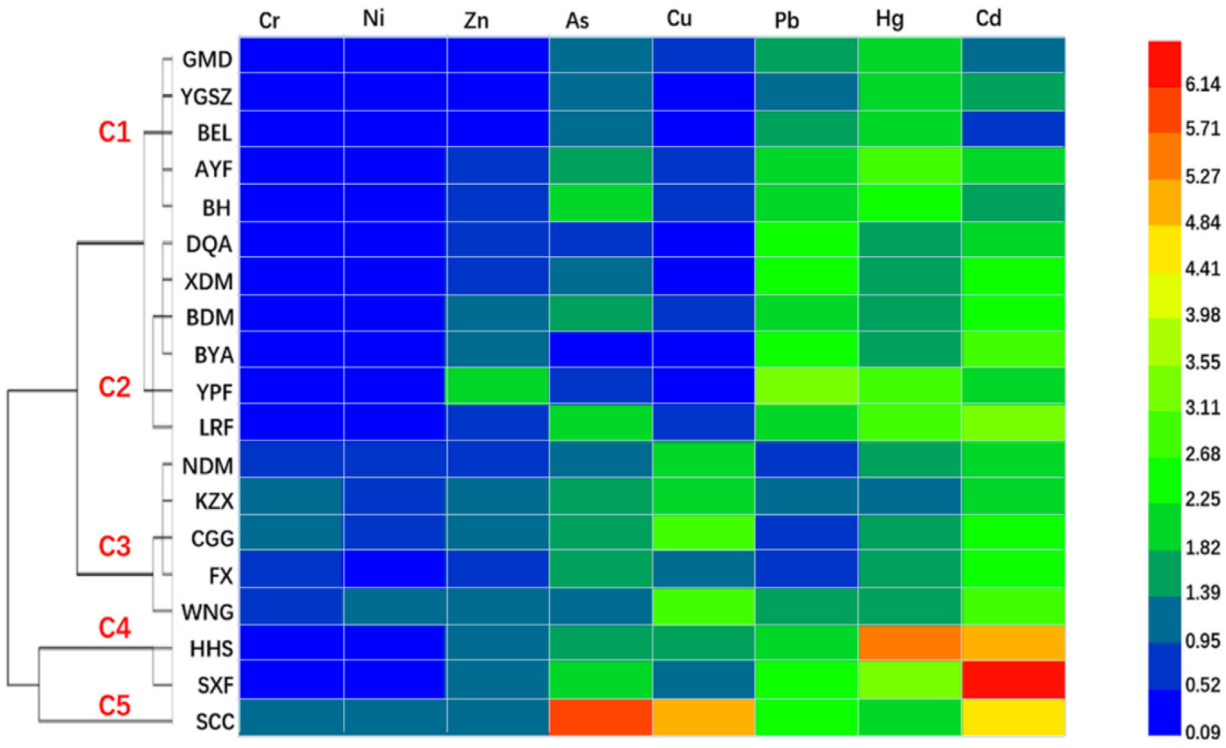

Fig. 2 – Hierarchical cluster analysis (HCA) heat maps of trace metal(loid)s in road soils, providing information of relationship among trace metal(loid)s and sites. Ward method and squared Euclidean correlation were used for clustering (left of the map), and the clustering results were divided into five main groups (C1-C5). The color intensity (log scale) in each panel showed the concentration of the certain metal(loid) in the site, referring to the color key at the right side. The name of the sites used the acronym of the local place names, such as FX which stands for Fuxi. The concentration used here is the normalized concentration (measured concentration / local value of the element in soil of the study area).

seen clearly in boxplots (Fig. 3a) that the maximum values of Cr and Ni were less than 0, which suggested all sites were practically unpolluted. Meanwhile, the minimum value of Hg was greater than 0, indicating all sites were at a polluted level. The class distributions of eight trace metal(loid)s in soils (Fig. 3b) revealed that the I_{geo} values of all soil samples for Hg and Cd ranged from Class 0 to Class 4. Among which, the pollution levels of both elements belonged to Class 3 and 4, were 30% and 9%, respectively. The overall degree of soil pollution with Hg and Cd was significantly higher than that of the other trace metal(loid)s.

Based on the Nemerow index, the mean, minimum and maximum values of PI of Cd (1.0, 0.33–3.03) and Hg (0.5, 0.27–1.2) were relatively high in road soils (Table 3 and Appendix A Table S5). The mean values of PI decreased in the following order: Cd > Hg > As > Zn > Cu > Ni > Pb > Cr. In terms of the class distribution of Cd and Hg, the PI > 0.5 (warning limit) were 87% and 35% in all samples, respectively (Fig. 3d), while all the samples were unpolluted with Cr (Class 0). For the integrated pollution of the entire study area, the IPI index suggested that the study area was in the precaution risk level (IPI = 0.94), and the PLI index indicated that it was in the slightly polluted level (PLI=1.13), based on the values and classification in Table 1 and Table 3. Among all trace metal(loid)s, Cd had the highest IPI pollution level of 2.26, and according to the classification criteria for pollution level, the soils were moderately polluted with Cd.

According to the ecological risk index, the trace metal(loid)s with potential ecological risks decreased in the order of Hg > Cd > As > Pb > Cu > Ni > Zn > Cr. The values of single potential ecological risk assessment of trace metal(loid)s (E_r^i) indicated that Cd and Hg were the two main contributors to ecological risks. This was because their assessment results were much greater than those of other trace metal(loid)s (Table 3). Hg had the greatest risk value of 216.78, which was followed by Cd of 97.85. The biological toxicity of Hg and Cd currently presented high and considerable potential for ecological risks, respectively, showing that they have a significant effect on the results of potential ecological risk assessment (RI). The RI value was 347.10, suggesting that the ecological risk level of the eight trace metal(loid)s in road soils of this study area was considerable.

2.3. *Source apportionment by combining PMF and PCA*

Firstly, the principal component analysis (PCA) and correlation analysis were used to preliminarily identify the potential sources of trace metal(loid)s in soils (Fig. 4). To reduce the number of highly loaded elements on each component, varimax rotation was used to Kaiser normalization for trace

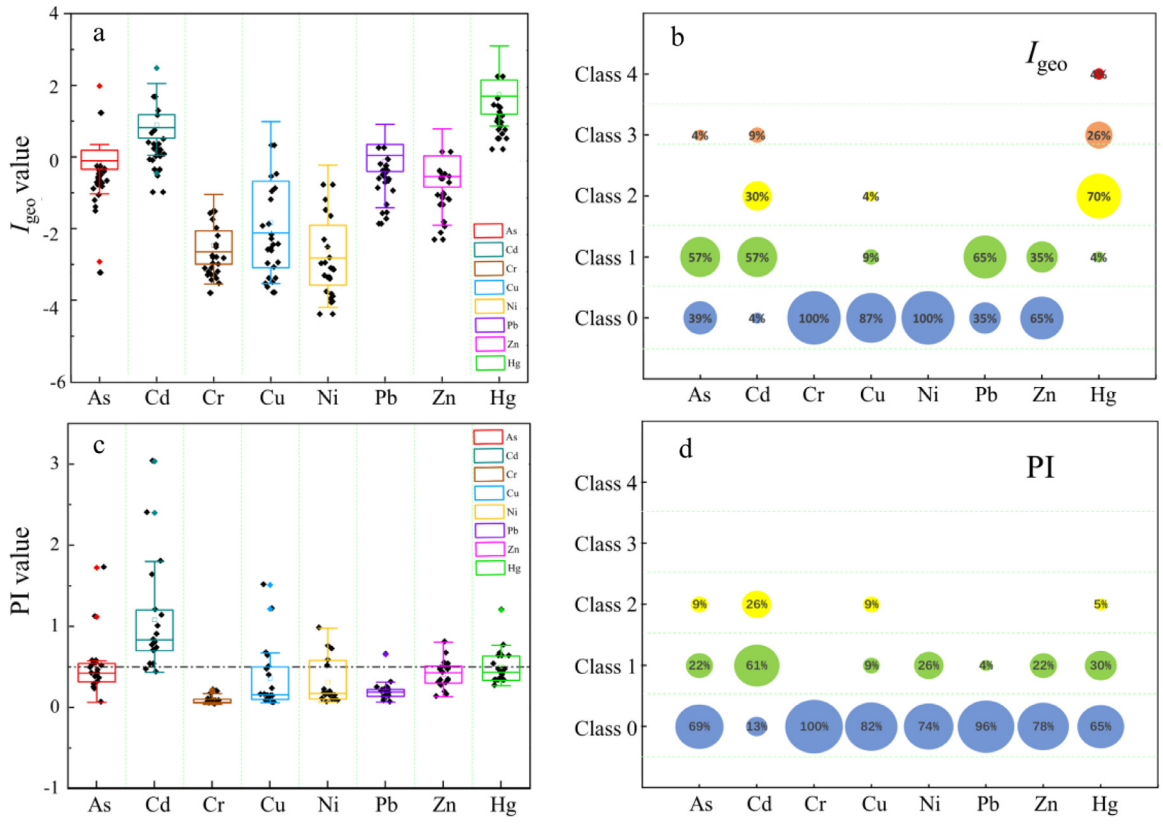

Fig. 3 – Boxplots (a, c) and class distribution (b, d) of the I_{geo} and PI values for the eight trace metal(loid)s in the study area. The black dashed horizontal line in boxplots presented the guideline values (0 for I_{geo} and 0.5 for PI).

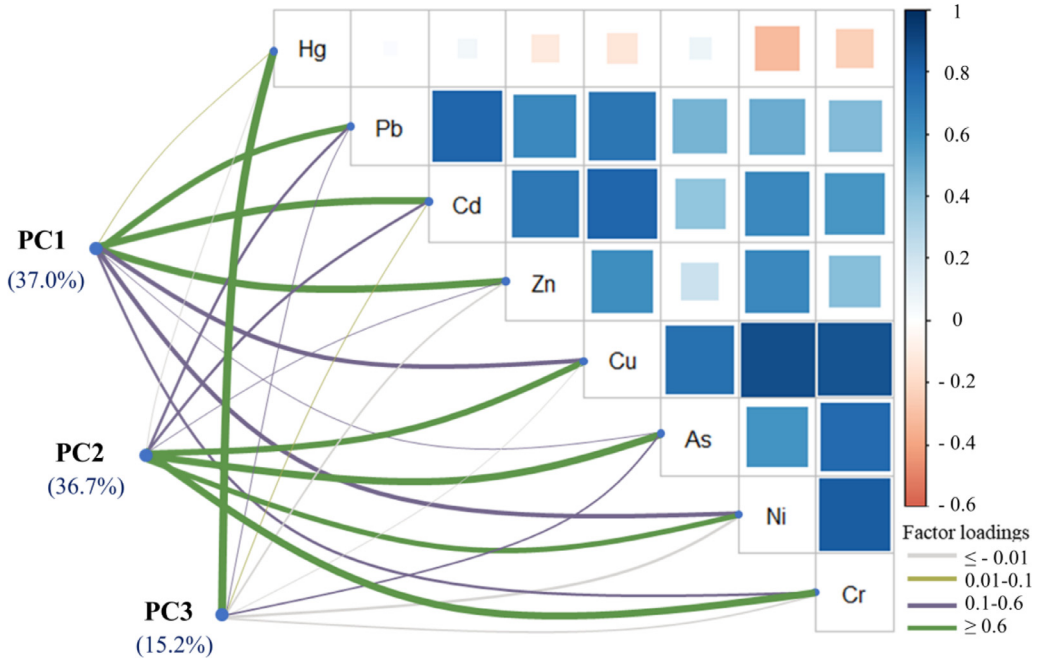

Fig. 4 – Identify the correlations between concentrations of trace metal(loid)s. Pairwise comparisons of trace metal(loid)s are shown, with a color gradient denoting Pearson correlation coefficients. Factor loadings for varimax rotated Principal component analysis (PCA) were related to each trace metal(loid). Edge color denotes the ranges of factor loadings, and edge width corresponds to the values of loading in proportion.

Table 3 – Results of I_{geo}, RI, PI, IPI, and PLI.

Indices		As	Cd	Cr	Cu	Ni	Pb	Zn	Hg
Geo-accumulation index	I_{geo}	−0.05±0.81*	0.97±0.65	−2.29±0.69	−1.72±1.24	−2.43±1.09	0.01±0.61	−0.43±0.67	1.78±0.05
Potential ecological	E_r^i	16.70±10.72	97.85±51.96	0.70±0.38	3.56±3.58	1.93±1.71	8.33±3.24	1.24±0.54	216.78±87.69
Risk index	RI	347.10±125.13							
Nemerow pollution index	PI	0.49±0.33	1 ± 0.66	0.09±0.05	0.32±0.38	0.29±0.26	0.19±0.12	0.38±0.17	0.5 ± 0.2
	IPI	0.94±0.63							
Pollution load index	PLI	1.13±0.45							

* Mean ± Standard Deviation.

metal(loid) concentrations in PCA (Zhang et al., 2018b). The detailed numerical results were given in Appendix A Tables S6 and S7. Based on the results of eigenvalues, PCA extracted three components (named as PC1, PC2 and PC3, respectively) which explained 88.9% of the cumulative variance, and their loading plots were presented in Fig. 5a. The PCA results indicated that PC1 mainly loaded on Cd, Pb and Zn, with a significant correlation between these trace metal(loid)s ($p < 0.01$) (Appendix A Table S6). PC2 was weighted heavily on As, Cr, Cu and Ni with high loadings (0.934, 0.882, 0.766 and 0.686, respectively), while PC3 was dominated by Hg with a high loading of 0.963. Strong correlations suggest a common source (Jin et al., 2019).

To more accurately identify the sources of the eight trace metal(loid)s and quantify their corresponding contributions in road soils of the study area, the PMF model was further used. The model fitting showed that the fitting coefficients (r^2) of all trace metal(loid)s were greater than 0.82 (Appendix A Fig. S2), indicating that the overall fitting effect between the observed and the predicted concentrations of the PMF model well explained the information included in the original data and the results were reliable (Zhang et al., 2018b). Ultimately, according to the PMF processing results, five factors (including Factor 1, Factor 2, Factor 3, Factor 4 and Factor 5) were identified (Fig. 5b and Appendix A Fig. S3). Comparing the results of PCA and PMF model, it was found that the PMF model provides a more detailed and quantifiable explanation for the sources of trace metal(loid)s in road soils, and the contributions of each source were showed in Fig. 5c.

Factor 1 which accounted for 10.53% of the contribution rate was dominated by Hg (78.5%, Fig. 5c). Previous studies have shown that the strong correlations of Pearson correlation coefficients suggest a common source (Ali et al., 2016; Jin et al., 2019). As shown in Fig. 4, because Hg had a low positive or even negative correlation with the other 7 trace metal(loid)s, it suggested that the pollution source of Hg might differ from other trace metal(loid)s (Zhang et al., 2018a). The average concentration of Hg (0.14 mg/kg) was moderately enriched in road soils as compared to background value (0.0675 mg/kg), and according to the I_{geo} and RI results of Hg, most sites were at polluted level indicating an anthropogenic source. Hg is an important element in fertilizers and pesticides with strong volatility and migration (Dong et al., 2017; Giersz et al., 2017), and can migrate into soil, water and atmosphere, leading to high Hg concentrations in these environmental media. Moreover, the spatial distribution analysis also shown that Hg pollution was widespread, and the western peripheral non-main scenic areas (C1 group) with a large amount of forestland were mainly controlled by Hg pollution (Fig. 2). Since this study area is surrounded by many famous tea-producing areas, Hg pollution may be attributed to the extensive use of Hg-containing pesticides and fertilizers for large-scale tea planting and greening care in and around the study area (Jiang, 2019; Men et al., 2018). Therefore, Factor 1 may originate from an agricultural source.

Factor 2 with a contribution rate of 34.02% was mainly loaded on Zn (52.4%) and Pb (43.3%), while Factor 3 with a contribution rate of 5.91% was mostly loaded on Cd (49.0%) (Fig. 5b and Appendix A Fig. S3). A growing number of studies have proved that the accumulation of Cd, Pb and Zn in soils and plants along roads were caused by traffic source

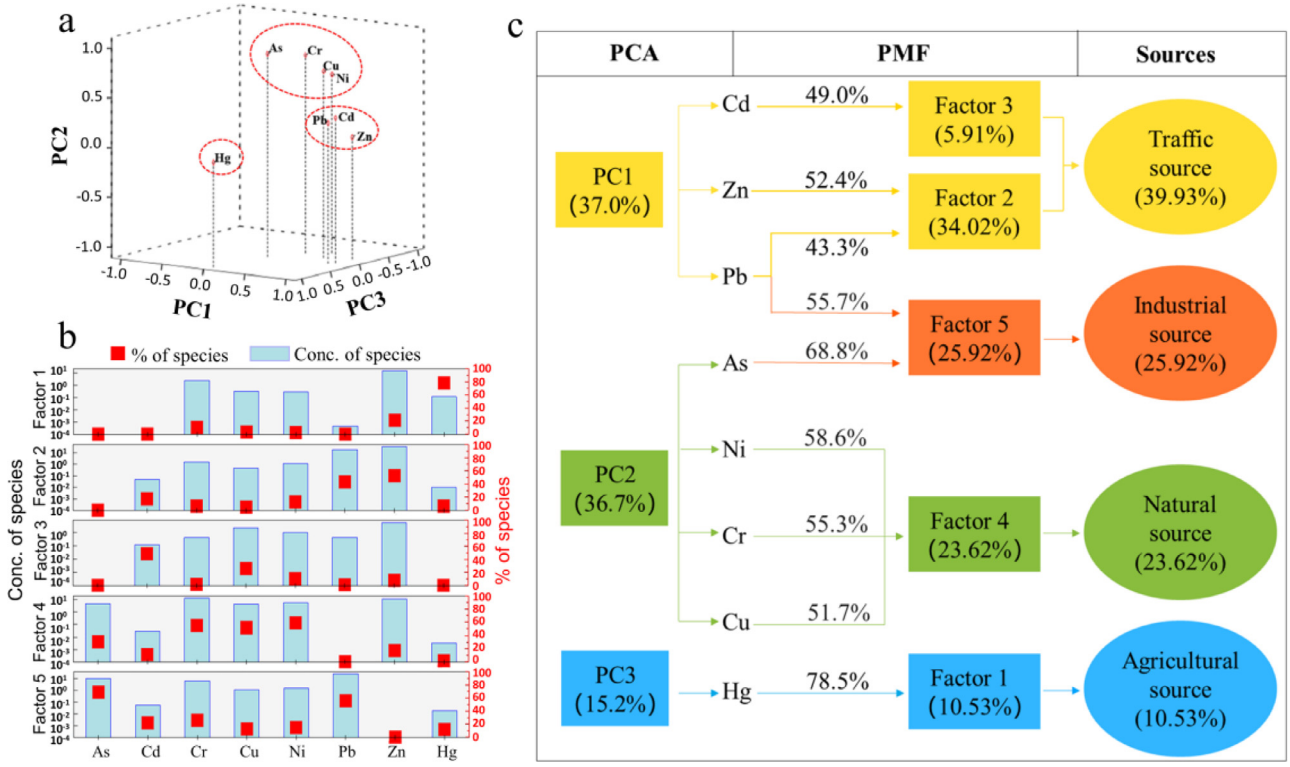

Fig. 5 – Apportion the potential sources of trace metal(loid)s. (a) Factors loadings for rotated components of the PCA; (b) the concentrations of species and source contributions from PMF model; (c) the source apportionment of trace metal(loid)s by the combination of qualitative (PCA) and quantitative analysis (PMF).

(Brtnicky et al., 2019; Dao et al., 2014; Jiang et al., 2017; Yanosky et al., 2012). It was reported that Cd is an important element contained in tires and lubricating oil (Duan and Tan, 2013), while Pb and Zn were mainly found in automobile exhaust (Zhang et al., 2016). Since the sampling sites were adjacent to the busy roads with heavy traffic, a higher concentration of Cd, Zn and Pb in this study area than their average background concentration in Anhui province suggests their probable source from the traffic emission. In addition, Cd, Zn and Pb are highly correlated ($p < 0.01$), which also indicates that they may have the same source (Appendix A Table S6). Hence, Factors 2 and 3 can be combined and attributed to traffic sources.

Factor 4, contributing 23.62%, was mainly supported by Ni (58.6%), Cr (55.3%) and Cu (51.7%). The correlations among Cr, Cu and Ni in the study area are statistically significant ($p < 0.01$), which suggested that they might share a common source (Appendix A Table S6). Previous studies indicated that the parent material and pedogenic process are the main contributors affecting the content of Cr and Ni (Lu et al., 2012, 2017; Madrid et al., 2002; Zhang et al., 2018b). The average concentrations of Cr, Cu and Ni were significantly lower than the background values of Anhui province, and according to the results of I_{geo} assessment (Fig. 3), there was no Cr and Ni pollution in road soils of the study area, and Cu was slightly polluted, showing no significant anthropogenic impact of these trace metal(loid)s. Thus, Factor 4 was identified as a natural source.

Factor 5, mainly loaded on As (68.8%) and Pb (55.7%), was considered as an industrial source. It was reported that As was commonly used as alloy additives, catalysts and some electroplated materials (Li et al., 2020). In addition, coal consumption was an important cause of human activity to As pollution (Liu et al., 2020). In this study, the average concentration of As was 13.68 mg/kg, exceeding the background value (8.4 mg/kg), and the high concentration of As was found in C5 group adjacent to coal and copper mining areas (Fig. 2), suggesting a potential anthropogenic source from industrial influence, such as smelting, mining activities and so on (Ma et al., 2018). Although Pb was the main element of traffic source associated with automobile emission, it was widely founded in wastewater discharges from mine tailing, smelting (Liao et al., 2017) and the production of Pb batteries as well (Urrutia Goyes et al., 2018). Therefore, Factor 5 was most probably associated with industrial sources.

2.4. *Human health risk assessment*

The health risks (including non-carcinogenic risk and carcinogenic risk) of adults and children posed by soil trace metal(loid)s through three exposure pathways were analyzed, and the results were shown in Table 4. The result of PMF was adopted to quantify the contribution of different sources to human health risks. Health risks caused by the apportioned sources were obtained by multiplying the health risk values of

Table 4 – Health risks to children and adults through different exposure pathways.

	Children				Adults			
	Ingestion	Inhalation	Dermal	Total risk	Ingestion	Inhalation	Dermal	Total risk
Non-carcinogenic risk (HI)								
As	5.09E-02	1.39E-04	3.48E-03	5.45E-02	2.97E-02	5.78E-04	2.89E-03	3.31E-02
Cd	7.21E-04	4.21E-06	2.02E-04	9.27E-04	4.20E-04	1.76E-05	1.68E-04	6.05E-04
Cr	1.87E-02	3.29E-05	2.62E-03	2.14E-02	1.09E-02	4.56E-04	2.18E-03	1.36E-02
Cu	9.77E-04	5.71E-08	9.12E-06	9.86E-04	5.70E-04	2.38E-07	7.58E-06	5.78E-04
Ni	1.41E-03	1.83E-05	1.46E-05	1.44E-03	8.21E-04	7.62E-05	1.21E-05	9.10E-04
Pb	3.26E-02	3.34E-05	6.09E-04	3.32E-02	1.90E-02	1.39E-04	5.06E-04	1.97E-02
Zn	6.07E-04	3.55E-08	8.50E-06	6.16E-04	3.54E-04	1.48E-07	7.07E-06	3.61E-04
Hg	1.20E-03	2.46E-07	4.80E-05	1.25E-03	7.00E-04	1.02E-06	3.99E-05	7.41E-04
Carcinogenic risk (CR)								
As	2.29E-05	3.61E-08	1.56E-06	2.45E-05	1.34E-05	1.51E-07	1.30E-06	1.49E-05
Cd	n/a	3.06E-10	n/a	3.06E-10	n/a	1.27E-09	n/a	1.27E-09
Cr	n/a	1.59E-07	n/a	1.59E-07	n/a	6.63E-07	n/a	6.63E-07
Ni	n/a	1.59E-09	n/a	1.59E-09	n/a	6.64E-09	n/a	6.64E-09
Pb	3.60E-07	3.23E-10	n/a	3.60E-07	4.89E-07	1.35E-09	n/a	4.91E-07

n/a: the data is not available because of the lack of relevant calculation parameters.

individual trace metal(loid)s by the contribution rates of identified sources (Ma et al., 2018) (Fig. 7).

The non-carcinogenic risk was evaluated by the total hazard index (HI), and all the HI values were lower than 1, which indicated that trace metal(loid)s of road soils in the study area posed no significant non-carcinogenic health risks to children or adults through the three pathways mentioned above. The HI values for children decreased in the order of As > Pb > Cr > Ni > Hg > Cu > Cd > Zn. However, compared with adults, the non-carcinogenic risk for children was significantly higher, showing that children were more susceptible to the eight trace metal(loid)s in the study area. In addition, the non-carcinogenic risk values for the trace metal(loid)s were 1–4 orders of magnitude higher for the ingestion pathway than for the inhalation pathway (Table 4), and the relative contribution of the ingestion pathway to the total risk of the trace metal(loid)s ranged from 77.77% to 99.07% for children and from 69.41% to 98.65% for adults (Fig. 6 and Appendix A Table S8). The result suggested that the ingestion of soil particles appeared to be more important than the other two exposure pathways through which health risks are posed to tourists, and the inhalation pathway contributed to the almost negligible risks. The main ingestion pathway might be in part because of incidental hand-to-mouth contact (Ma et al., 2018). This result was consistent with previous studies (Gu et al., 2016; Yang et al., 2018). Therefore, it is quite necessary to instruct children to take protective measures, such as wash hands frequently or wear protective gloves to reduce the risks through ingestion and dermal contact pathways when they play in the national park.

As shown in Table 4, the total carcinogenic risk values of As, Cd, Cr, Ni and Pb for children from ingestion, inhalation and dermal decreased in the order of As > Pb > Cr > Ni > Cd. It is generally considered that if the value of total risk exceeds the limit (1×10^{-4}), it indicates a significant risk of cancer effects; and if the value is lower than 1×10^{-6}, it indicates negligible cancer risk effects (Tepanosyan et al., 2017; USEPA, 2009). The carcinogenic risks for As, Cd, Cr, Ni and Pb through inhalation exposure pathway were all significantly lower than 1×10^{-6}, indicating negligible inhalation carcinogenic risks in this area. However, CR values of As for children and adults through ingestion and dermal contact were higher than the limit value of 1×10^{-6}, indicating As pollution in park road soils should be paid more attention to protecting human health from carcinogenic risk.

The contribution rates of different sources to the non-carcinogenic risks and carcinogenic risks were similar among children and adults (Fig. 7 and Appendix A Fig. S4), which was consistent with the previous study (Ma et al., 2018). Hence, only the health risks of adults were discussed here. As shown in Fig. 7, the industrial and traffic sources were the two most important anthropogenic sources of the health risks for adults, with non-carcinogenic risks accounting for 52.72% and 24.76%, and the carcinogenic risks accounting for 65.14% and 4.14%, respectively. It indicated that industrial and traffic sources could pose significant impacts on human health risks, with the industrial source was mostly characterized by Pb and As, and traffic source was mainly loaded on Cd, Zn and Pb. Therefore, to reduce the health risks for tourists in the na-

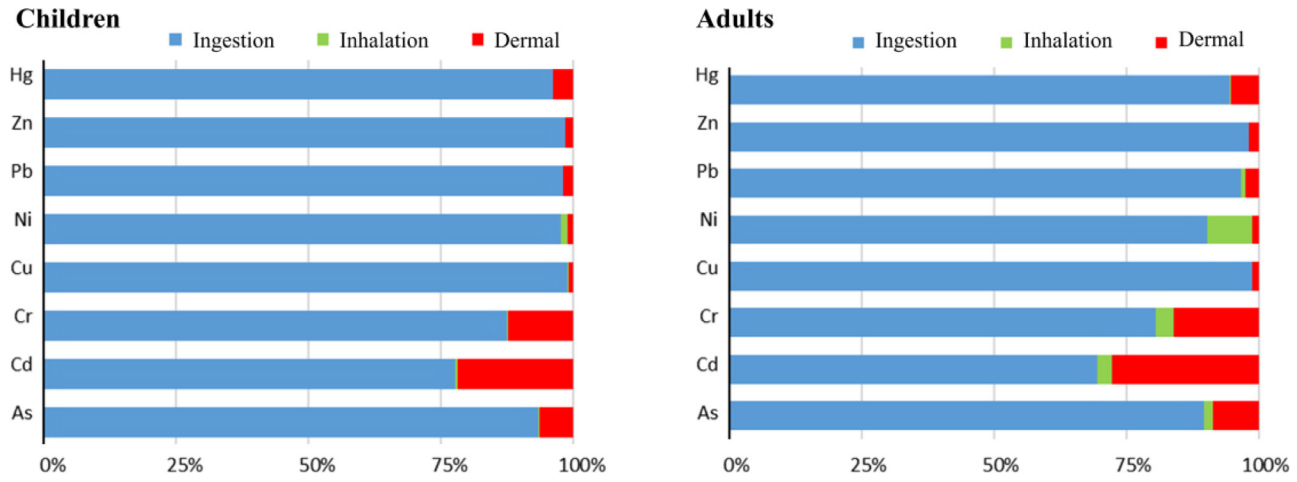

Fig. 6 – Relative contributions to the hazard index (HI) for each metal(loid) through three exposure pathways (ingestion, inhalation, and dermal exposure).

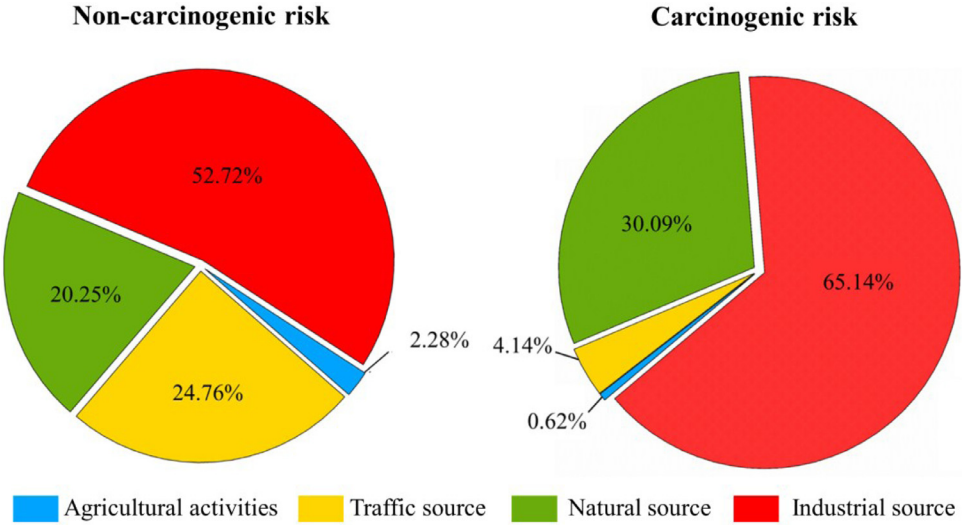

Fig. 7 – Contributions of each source to the health risks for adults.

tional parks, it is essential to consider predominant sources in health risk assessment.

Conclusions

In conclusion, to explore the pollution levels, potential sources and health risks of trace metal(loid)s in road soils, a highly-visited national park was investigated. Results showed that Hg and Cd were the most accumulated elements in road soils of the study area, and the pollution of trace metal(loid)s mainly originated from traffic, industrial, agricultural and natural sources. The PMF model provided a more detailed and quantifiable explanation for the sources of trace metal(loid)s in road soils compared with PCA. However, the combination of these two models can well apportion the pollution sources qualitatively and quantitatively.

According to the results of the health risk assessment, through inhalation, ingestion or dermal pathways, the trace metal(loid)s posed no obvious non-carcinogenic health risks to children or adults. However, industrial and traffic sources seriously affected the health risks, indicating risk control should be given priority to these sources. Model results are closely related to the selection of parameters and the determination of parameter values. Therefore, to reduce the uncertainty of the risk assessment results, optimizing the model and conducting a more extensive investigation of exposure factors (such as exposure frequency, soil intake rate and skin adhesion factors) for different regions will be the focus of our follow-up research.

Acknowledgments

This work was supported by the Major Project of the National Social Science Foundation of China (No. 14ZDB140). We would like to express our thanks to the anonymous reviewers for their helpful comments on the manuscript.

REFERENCES

Ali, M.H., Mustafa, A.-R.A., El-Sheikh, A.A., 2016. Geochemistry and spatial distribution of selected heavy metals in surface soil of Sohag, Egypt: a multivariate statistical and GIS approach. Environ. Earth. Sci. 75, 1–17.

Bocca, B., Alimonti, A., Petrucci, F., Violante, N., Sancesario, G., Forte, G., et al., 2004. Quantification of trace elements by sector field inductively coupled plasma mass spectrometry in urine, serum, blood and cerebrospinal fluid of patients with Parkinson's disease. Spectrochim. Acta 59, 559–566.

Brtnicky, M., Pecina, V., Hladky, J., Radziemska, M., Koudelkova, Z., Klimanek, M., et al., 2019. Assessment of phytotoxicity, environmental and health risks of historical urban park soils. Chemosphere 220, 678–686.

Caeiro, S., Costa, M.H., Ramos, T.B., Fernandes, F., Silveira, N., Coimbra, A., et al., 2005. Assessing heavy metal contamination in Sado Estuary sediment: an index analysis approach. Ecol. Indic. 5, 151–169.

CNEM (China National Environmental Monitoring Centre)„ 1990. Background concentrations of elements in soils of China (in Chinese). China Environ. Sci. Press, Beijing 329–501.

Chen, H., Teng, Y., Lu, S., Wang, Y., Wang, J., 2015. Contamination features and health risk of soil heavy metals in China. Sci. Total. Environ. 512, 143–153.

Chen, R., Chen, H., Song, L., Yao, Z., Meng, F., Teng, Y., 2019. Characterization and source apportionment of heavy metals in the sediments of Lake Tai (China) and its surrounding soils. Sci. Total. Environ. 694, 133819.

Cheng, H., Li, M., Zhao, C., Li, K., Peng, M., Qin, A., et al., 2014. Overview of trace metals in the urban soil of 31 metropolises in China. J. Geochem. Explor. 139, 31–52.

Dao, L., Morrison, L., Zhang, H., Zhang, C., 2014. Influences of traffic on Pb, Cu and Zn concentrations in roadside soils of an urban park in Dublin. Ireland. Environ. Geochem. Hlth. 36, 333–343.

Dong, H., Lin, Z., Wan, X., 2017. Risk assessment for the mercury polluted site near a pesticide plant in Changsha, Hunan, China. Chemosphere 169, 333–341.

Duan, J., Tan, J., 2013. Atmospheric heavy metals and Arsenic in China: situation, sources and control policies. Atmos. Environ. 74, 93–101.

Elmira, S., Vesna, M., Dragan, Č., Darko, J., Veljko, P., Svetlana, A.M., et al., 2019. Pollution indices and sources appointment of heavy metal pollution of agricultural soils near the thermal power plant. Environ. Geochem. Hlth. 41, 2265–2279.

Gao, J., Wang, L.C., 2018. Ecological and human health risk assessments in the context of soil heavy metal pollution in a typical industrial area of Shanghai. China. Environ. Sci. Pollut. R. 25, 27090–27105.

Gasiorek, M., Kowalska, J., Mazurek, R., Pajak, M., 2017. Comprehensive assessment of heavy metal pollution in topsoil of historical urban park on an example of the Planty Park in Krakow (Poland). Chemosphere 179, 148–158.

Giersz, J., Bartosiak, M., Jankowski, K., 2017. Sensitive determination of Hg together with Mn, Fe, Cu by combined photochemical vapor generation and pneumatic nebulization in the programmable temperature spray chamber and inductively coupled plasma optical emission spectrometry. Talanta 167, 279–285.

Gonzalez, M.J., Fernandez, M., Hernandez, L.M., 1990. Influence of acid mine water in the distribution of heavy metal in soils of Donana national park. Application of multivariate analysis. Environ. Technol. 11, 1027–1038.

Gu, Y.G., Lin, Q., Gao, Y.P., 2016. Metals in exposed-lawn soils from 18 urban parks and its human health implications in southern China's largest city. Guangzhou. J. Clean. Prod. 115, 122–129.

Guan, Q.Y., Wang, F.F., Xu, C.Q., Pan, N.H., Lin, J.K., Zhao, R., et al., 2018. Source apportionment of heavy metals in agricultural soil based on PMF: a case study in Hexi Corridor, northwest China. Chemosphere 193, 189–197.

Hakanson, L., 1980. An ecological risk index for aquatic pollution control.a sedimentological approach. Water Res 14, 975–1001.

Hamad, R., Balzter, H., Kolo, K., 2019. Assessment of heavy metal release into the soil after mine clearing in Halgurd-Sakran National Park, Kurdistan, Iraq. Environ. Sci. Pollut. R. 26, 1517–1536.

Huang, J.H., Guo, S.T., Zeng, G.M., Li, F., Gu, Y.L., Shi, Y.H., et al., 2018. A new exploration of health risk assessment quantification from sources of soil heavy metals under different land use. Environ. Pollut. 243, 49–58.

Hung, W.C., Hernandez-Cira, M., Jimenez, K., Elston, I., Jay, J.A., 2018. Preliminary assessment of lead concentrations in topsoil of 100 parks in Los Angeles, California. Appl. Geochem. 99, 13–21.

Irzon, R., Syafri, I., Hutabarat, J., Sendjaja, P., Permanadewi, S., 2018. Heavy metals content and pollution in tin tailings from Singkep Island, Riau, Indonesia. Sains Malays 47, 2609–2616.

Jiang, N., 2019. Research on the improvement of the core competitiveness of tea industry in famous tea town: a case study of Huangshan City, Anhui Province. IOP Conf. Ser.: Earth Environ. Sci. 346, 012082.

Jiang, Y., Chao, S., Liu, J., 2017. Source apportionment and health risk assessment of heavy metals in soil for a township in Jiangsu Province. China. Chemosphere. 168, 1658–1668.

Jin, Y.L., O'Connor, D., Ok, Y.S., Tsang, D.C.W., Liu, A., Hou, D.Y., 2019. Assessment of sources of heavy metals in soil and dust at children's playgrounds in Beijing using GIS and multivariate statistical analysis. Environ. Int. 124, 320–328.

Khan, S., Munir, S., Sajjad, M., Li, G., 2016. Urban park soil contamination by potentially harmful elements and human health risk in Peshawar City, Khyber Pakhtunkhwa, Pakistan. J. Geochem. Explor. 165, 102–110.

Li, J., Jia, C., Lu, Y., Tang, S., Shim, H., 2015. Multivariate analysis of heavy metal leaching from urban soils following simulated acid rain. Microchem. J. 122, 89–95.

Li, X., Feng, L., 2012. Multivariate and geostatistical analyzes of metals in urban soil of Weinan industrial areas, Northwest of China. Atmos. Environ. 47, 58–65.

Li, Y., Yuan, Y., Sun, C., Sun, T., Liu, X., Li, J., et al., 2020. Heavy metals in soil of an urban industrial zone in a metropolis: risk assessment and source apportionment. Stoch. Env. Res. Risk. A. 34, 435–446.

Liao, J., Chen, J., Ru, X., Chen, J., Wu, H., Wei, C., 2017. Heavy metals in river surface sediments affected with multiple pollution sources, South China: distribution, enrichment and source apportionment. J. Geochem. Explor. 176, 9–19.

Liu, J., Liu, Y.J., Liu, Y., Liu, Z., Zhang, A.N., 2018. Quantitative contributions of the major sources of heavy metals in soils to ecosystem and human health risks: a case study of Yulin. China. Ecotox. Environ. Safe. 164, 261–269.

Liu, L., Liu, Q., Ma, J., Wu, H., Qu, Y., Gong, Y., et al., 2020. Heavy metal(loid)s in the topsoil of urban parks in Beijing, China: concentrations, potential sources, and risk assessment. Environ. Pollut. 260, 114083.

Lu, A., Wang, J., Qin, X., Wang, K., Han, P., Zhang, S., 2012. Multivariate and geostatistical analyses of the spatial distribution and origin of heavy metals in the agricultural soils in Shunyi, Beijing, China. Sci. Total. Environ. 425, 66–74.

Lu, J., Li, A., Huang, P., 2017. Distribution, sources and contamination assessment of heavy metals in surface sediments of the South Yellow Sea and northern part of the East China Sea. Mar. Pollut. Bull. 124, 470–479.

Ma, W., Tai, L., Qiao, Z., Zhong, L., Wang, Z., Fu, K., et al., 2018. Contamination source apportionment and health risk

assessment of heavy metals in soil around municipal solid waste incinerator: a case study in North China. Sci. Total. Environ. 631, 348–357.
Madrid, L., Díaz-Barrientos, E., Madrid, F., 2002. Distribution of heavy metal contents of urban soils in parks of Seville. Chemosphere 49, 1301–1308.
Marchand, C., Allenbach, M., Lallier-Vergès, E., 2011. Relationships between heavy metals distribution and organic matter cycling in mangrove sediments (Conception Bay, New Caledonia). Geoderma 160, 444–456.
Mazurek, R., Kowalska, J., Gasiorek, M., Zadrozny, P., Jozefowska, A., Zaleski, T., et al., 2017. Assessment of heavy metals contamination in surface layers of Roztocze National Park forest soils (SE Poland) by indices of pollution. Chemosphere 168, 839–850.
Mazurek, R., Kowalska, J.B., Gąsiorek, M., Zadrożny, P., Wieczorek, J., 2019. Pollution indices as comprehensive tools for evaluation of the accumulation and provenance of potentially toxic elements in soils in Ojców National Park. J. Geochem. Explor. 201, 13–30.
Meharg, A.A., 2011. Trace Elements in Soils and Plants. 4th Ed. Exp. Agr. 47, 739.
Memoli, V., De Marco, A., Esposito, F., Panico, S.C., Barile, R., Maisto, G., 2019. Seasonality, altitude and human activities control soil quality in a national park surrounded by an urban area. Geoderma 337, 1–10.
Men, C., Liu, R., Xu, F., Wang, Q., Guo, L., Shen, Z., 2018. Pollution characteristics, risk assessment, and source apportionment of heavy metals in road dust in Beijing. China. Sci. Total. Environ. 612, 138–147.
Mrimi, D.J., Nyahongo, J.W., Vedeld, P.O., Massawe, B.H., Jjunju, C.N., 2019. Spatial distribution of heavy metals in soil with distance from Tazama pipeline through the Mikumi National Park. Tanzania. J. Soil Sci. Environ. Manag. 10, 75–81.
Paatero, P., 1994. Positive matrix factorization: a non-negative factor model with optimal utilization of error estimates of data values. Environmetrics 5, 111–126.
Paatero, P., 1997. Least squares formulation of robust non-negative factor analysis. Chemometr. Intell. Lab. 37, 23–35.
Paatero, P., Tapper, U., 1993. Analysis of different modes of factor analysis as least squares fit problems. Chemometr. Intell. Lab. 18, 183–194.
Parzych, A., 2014. The heavy metal content of soil and shoots of *Vaccinium myrtillus* L. in the Słowiński National Park. Forest Res. Papers. 75, 217–224.
Ratko, K., Snezana, B., Dragica, O., Ivana, B., Nada, D., 2011. Assessment of heavy metal content in soil and grasslands in national park of the lake plateau of the N. P. "Durmitor" Montenegro. Afr. J. Biotechnol. 10, 5157–5165.
Saglam, C., 2017. Heavy metal concentrations in serpentine soils and plants from Kizildag National Park (Isparta) in Turkey. Fresen. Environ. Bull. 26, 3995–4003.
Shao, X., Wu, M., Jiang, K., 2007. Distribution and ecological risk assessment of heavy metal elements in soils of Xixi Wetland. Wetland Sci 3, 253–259.
Tepanosyan, G., Sahakyan, L., Belyaeva, O., Maghakyan, N., Saghatelyan, A., 2017. Human health risk assessment and riskiest heavy metal origin identification in urban soils of Yerevan. Armenia. Chemosphere. 184, 1230–1240.
Tian, S.H., Liang, T., Li, K.X., Wang, L.Q., 2018. Source and path identification of metals pollution in a mining area by PMF and rare earth element patterns in road dust. Sci. Total. Environ. 633, 958–966.
Urrutia Goyes, R., Argyraki, A., Ornelas Soto, N., 2018. Characterization of soil contamination by lead around a former battery factory by applying an analytical hybrid method. Environ. Monit. Assess. 190, 429.
USEPA, 2009. Risk Assessment Guidance for Superfund (RAGS). U.S. Environment Protection Agency, Washington, DC.
Waisberg, M., Joseph, P., Hale, B., Beyersmann, D., 2003. Molecular and cellular mechanisms of cadmium carcinogenesis. Toxicology 192, 95–117.
Wang, L.N., Chang, J., Zheng, X.R., Liu, J., Yu, M.Z., Liu, L.L., et al., 2018. Survey of ecological environmental conditions and influential factors for public parks in Shanghai. Chemosphere 190, 9–16.
Weissmannová, H.D., Pavlovský, J., 2017. Indices of soil contamination by heavy metals – methodology of calculation for pollution assessment (minireview). Environ. Monit. Assess. 189, 1–25.
Wu, S.H., Zhou, S.L., Bao, H.J., Chen, D.X., Wang, C.H., Li, B.J., et al., 2019. Improving risk management by using the spatial interaction relationship of heavy metals and PAHs in urban soil. J. Hazard. Mater. 364, 108–116.
Yang, Q., Li, Z., Lu, X., Duan, Q., Huang, L., Bi, J., 2018. A review of soil heavy metal pollution from industrial and agricultural regions in China: pollution and risk assessment. Sci. Total. Environ. 642, 690–700.
Yang, S., Zhao, J., Chang, S.X., Collins, C., Xu, J., Liu, X., 2019. Status assessment and probabilistic health risk modeling of metals accumulation in agriculture soils across China: a synthesis. Enviro. Int. 128, 165–174.
Yanosky, J.D., Tonne, C.C., Beevers, S.D., Wilkinson, P., Kelly, F.J., 2012. Modeling exposures to the oxidative potential of PM10. Environ. Sci. Technol. 46, 7612–7620.
Yaşar Korkanç, S., 2014. Impacts of recreational human trampling on selected soil and vegetation properties of Aladag Natural Park. Turkey. Catena. 113, 219–225.
Zhang, H., Mao, Z., Huang, K., Wang, X., Cheng, L., Zeng, L., et al., 2019. Multiple exposure pathways and health risk assessment of heavy metal(loid)s for children living in fourth-tier cities in Hubei Province. Enviro. Int. 129, 517–524.
Zhang, P., Qin, C., Hong, X., Kang, G., Qin, M., Yang, D., et al., 2018a. Risk assessment and source analysis of soil heavy metal pollution from lower reaches of Yellow River irrigation in China. Sci. Total. Environ. 633, 1136–1147.
Zhang, X.W., Wei, S., Sun, Q.Q., Wadood, S.A., Guo, B.L., 2018b. Source identification and spatial distribution of arsenic and heavy metals in agricultural soil around Hunan industrial estate by positive matrix factorization model, principle components analysis and geo statistical analysis. Ecotox. Environ. Safe. 159, 354–362.
Zhang, Y., Cao, S., Xu, X., Qiu, J., Chen, M., Wang, D., et al., 2016. Metals compositions of indoor PM2.5, health risk assessment, and birth outcomes in Lanzhou. China. Environ. Monit. Assess. 188, 325.